

A simulation study for the effect of diffractive collisions on the air shower developments

Ken Ohashi^{*a}, Hiroaki Menjo^a, Yoshitaka Itow^{ab}, Takashi Sako^c, and Katsuaki Kasahara^d

^a *Institute for Space-Earth Environmental Research, Nagoya University, Nagoya, Japan*

^b *Kobayashi-Maskawa Institute, Nagoya University, Nagoya, Japan*

^c *Institute for Cosmic Ray Research, the University of Tokyo, Kashiwa, Japan*

^d *Shibaura Institute of Technology, Tokyo, Japan*

E-mail: ohashi.ken@isee.nagoya-u.ac.jp

The mass composition of ultra-high energy cosmic rays is important to understand their origin. The maximum depth of air shower developments, X_{max} , is one of the indicators of the mass composition. However, the prediction of X_{max} depends on the choice of the hadronic interaction model, which makes it difficult to interpret the mass composition. Diffractive collision is a collision type of hadronic interactions and one of the proposed sources of this uncertainty. In this study, we estimate the effect of the fraction of the diffractive collision on the prediction of the mean of X_{max} for the 10^{19} eV proton incident case by using air shower simulation package CONEX 5.64 and by artificially modifying the fraction of the diffractive collisions in the air shower simulation. The effect of the fraction difference among the major interaction models is estimated to be 8.9 g/cm^2 , which is non-negligible. Furthermore, we demonstrate that even if the same fraction of diffractive collisions is used in the models, the discrepancy between the current models in the X_{max} prediction does not reduce. Other sources of model discrepancy such as particle production after diffractive collisions must be studied more carefully.

*36th International Cosmic Ray Conference -ICRC2019-
July 24th - August 1st, 2019
Madison, WI, U.S.A.*

*Speaker.

1. Introduction

To understand the origin of ultra-high energy cosmic rays, it is important to measure mass composition. The maximum depth of the air shower developments, X_{max} , is an indicator of the mass composition used in ultra-high energy cosmic-ray observations. Heavier nuclei, such as iron nuclei, show a smaller value of the mean of X_{max} than lighter nuclei. Therefore, we can discriminate, for example, cosmic-ray protons and irons by comparing X_{max} observed by ultra-high energy cosmic-ray experiments and the X_{max} predictions by a Monte Carlo (MC) simulations. However, discrepancies in X_{max} predictions due to the choice of hadronic interaction models make it difficult to interpret the mass compositions from observations [1]. The source of the uncertainty of mass composition caused by hadronic interaction models needs to be elucidated for precisely understanding the mass composition.

Diffractive collision is a collision type of hadronic interactions and one of the proposed sources of this uncertainty. Diffractive collisions have four types, projectile single-diffractive collisions (projectile SD), target single-diffractive collisions (target SD), double-diffractive collisions (DD), and central-diffractive collisions (CD). Projectile SD is the collision type at which a projectile cosmic ray dissociates, whereas the target air nucleus does not change. In target SD, a target air nucleus dissociates, whereas the projectile cosmic ray does not change. In DD, both target air nucleus and projectile cosmic ray dissociate, and in CD, both are scattered, but some particles are produced. In this study, inelastic collisions other than diffractive collisions are called non-diffractive collisions (ND). Different types of collision have different effects on X_{max} predictions. If the collision type of the first interaction in the air shower is target SD or CD, for example, X_{max} predictions are one interaction length larger than that of the ND case because the projectile cosmic ray does not change in that collision. For projectile SD and DD cases, the number of produced particles in the collision is smaller and the energy of produced particles is larger than the ND case, which leads to larger X_{max} predictions.

The effects of diffractive collisions on the air shower developments were discussed in previous studies [2, 3]; however, the realistic effects of the detailed characteristics of diffractive collisions, such as the fraction of diffractive collision types, on air shower developments are not well understood yet. In this study, we estimate the effect of the fraction of diffractive collision types on the predictions of the mean of X_{max} , $\langle X_{max} \rangle$, by using the air shower simulation package CONEX 5.64 [4]. In Section 3, we discuss in detail the fraction of collision types and the relations between collision type and $\langle X_{max} \rangle$ predictions to understand which parameter affects $\langle X_{max} \rangle$ predictions. The effects of diffractive collisions are estimated in Section 4, and we provide conclusions in Section 5.

2. Simulation setup

In this work, we use the air shower simulation package CONEX 5.64 [4]. For studying the diffractive collisions in air showers, we modified CONEX in two ways: first, CONEX output was modified to provide the collision type at the first interaction in the air shower. Second, resampling by using collision types was added to modify the ratio among collision types for the whole air shower. The details of the latter modification are described in Section 4.2. The primary particles

are 10^{19} eV protons, and the zenith angle of these particles is 60° . For each of the three high-energy hadronic interaction models, EPOS-LHC [5], QGSJET II-04 [6], and SIBYLL 2.3c [7, 8], 40,000 events are generated. UrQMD v1.3.1 [9] is used for low-energy hadronic interactions below 80 GeV. For the definition of collision types, we use information of each hadronic interaction model. This definition is the same as in a previous study [3].

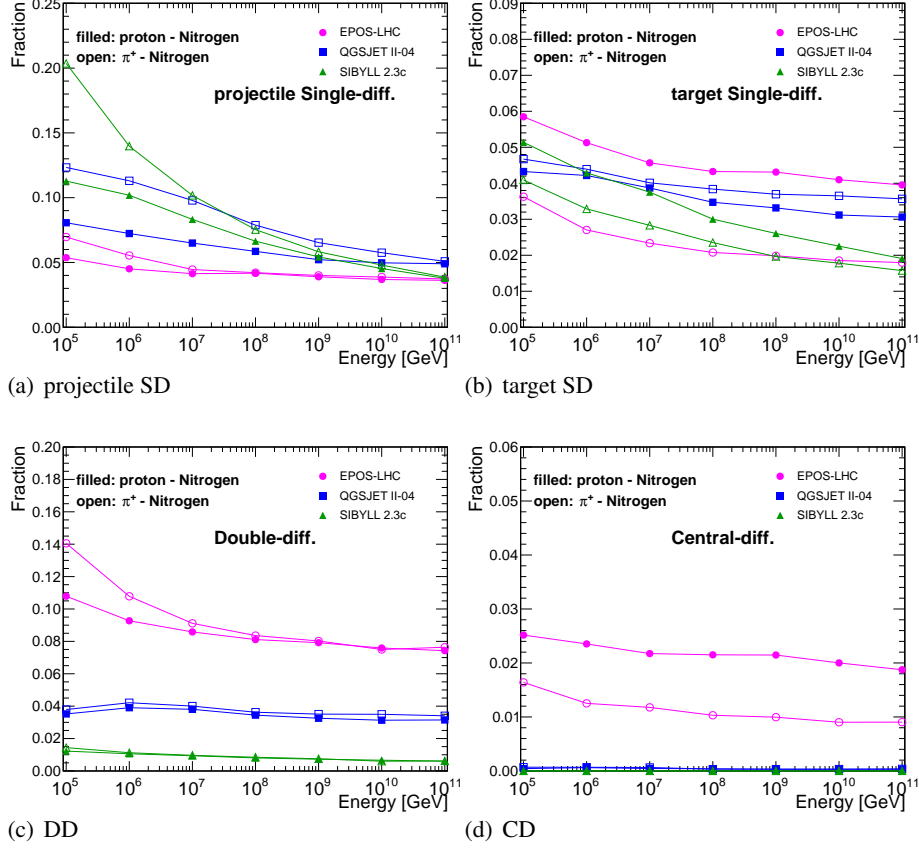


Figure 1: The fraction of collision types: (a) projectile SD, (b) target SD, (c) DD, and (d) CD simulated by using CRMC v1.7 [10]

3. The fraction of collision types and the relation to X_{max}

Before estimating the effect of diffractive collisions, we focus on the fraction of the collision types to understand which parameter affects X_{max} predictions. First, we check the fraction of the collision types for proton-Nitrogen and π^+ -Nitrogen collisions over a wide incident energy range using the event generator interface CRMC v1.7 [10]. Figure 1 shows the results of the fraction, which show the large model discrepancies in the fractions of diffractive collision types. These discrepancies can be the source of the model discrepancies of X_{max} predictions. As shown in Fig. 1 (a)(b), the fractions of the projectile SD and target SD depend on the incident energy, the incident particle, *i.e.* proton or π^+ , and the interaction model. In contrast, as seen in Fig. 1 (c), dependence in the incident particles is small in DD. The fraction of CD is very small in QGSJET II-04 and SIBYLL 2.3c, as seen in Fig. 1 (d).

Next, to understand the relation between collision type and X_{max} prediction, we categorize the events by the collision type of the first interaction in the air shower and calculate $\langle X_{max} \rangle$ predictions for each category. This categorization using information of the first interaction allows us to understand the effect of collision types in the simplest way. Figure 2 (a) shows the result of $\langle X_{max} \rangle$ of each category. $\langle X_{max} \rangle$ predictions of categories of diffractive collisions are larger than those of ND, and that of target SD is the largest among the categories. These results mean that the following two factors affect the model uncertainties of $\langle X_{max} \rangle$ predictions:

- The different modeling of particle production in the diffractive collisions, and
- The difference of the fraction of collision types.

Figure 2 (b) shows the differences of $\langle X_{max} \rangle$ among the categories. The differences between diffractive collisions and ND are 30 to 50 g/cm^2 , while those between DD and projectile SD are almost zero consistently. These results mean that the ratio of the fraction of projectile SD to DD does not affect the $\langle X_{max} \rangle$ predictions, while other ratios, such as the ratio of the fraction of diffractive collisions to ND or target SD to total SD, affect $\langle X_{max} \rangle$ predictions because of the differences between $\langle X_{max} \rangle$ predictions among the categories. Figure 2 (c) shows the differences of $\langle X_{max} \rangle$ among the models. The discrepancies among models are almost the same between ND and target SD. This is because a projectile proton does not change in target SD, so $\langle X_{max} \rangle$ becomes one interaction length larger than ND. The discrepancies in $\langle X_{max} \rangle$ predictions of ND and target SD among the models are larger than those of projectile SD and DD. The different modeling of diffractive collisions affects the discrepancies in the projectile SD and DD cases, while that of non-diffractive collisions affects ND and target SD cases, so these results mean that the effect of different modeling of diffractive collisions is smaller than that of non-diffractive collisions.

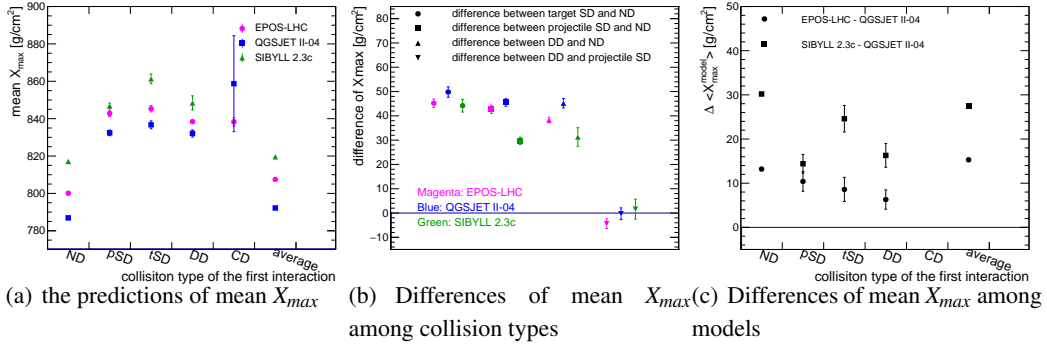


Figure 2: The prediction of mean X_{max} of each category for three hadronic interaction models (a) and its differences among categories (b) and among models (c). The differences among models $\Delta \langle X_{max}^{model} \rangle$ is mean X_{max} of EPOS-LHC or SIBYLL 2.3c subtracted by that of QGSJET II-04. The horizontal axes of (a) and (c) denote the collision type of the first interaction and the average of the collision types. Here, pSD means projectile SD and tSD means target SD.

In this study, we focus on the effect of differences of the fraction of collision types among the models. Because the discrepancies of $\langle X_{max} \rangle$ predictions of projectile SD and DD among the models are not so large, the effect of different modellings of diffractive collisions is not expected

to be very large, while the effect of the fraction is not well understood yet. Therefore, we estimate the effect of the fraction quantitatively in the next section.

4. The effect of the fraction of diffractive collisions on $\langle X_{max} \rangle$

4.1 The effect of diffractive collision at the first interaction on $\langle X_{max} \rangle$

To estimate the effect of the fraction at the first interaction in the air shower, we changed the ratios of the collision type at the first interaction within the range of the model-to-model variation. The cross-section fraction of each collision type to the total inelastic cross section is defined as f . To vary the f values, we introduced the following four parameters R_i . R_1 is the ratio of all diffractive collisions to the total inelastic collisions, R_2 is the ratio of SD collisions to sum of SD and DD, and R_3 is the ratio of target SD to SD. R_4 is the ratio of CD to all diffractive collisions. f can be calculated from these four ratios as shown in Equations 4.1,

$$\begin{aligned} f^{ND} &= 1 - R_1, \\ f^{projectile\ SD} &= R_1(1 - R_4)R_2(1 - R_3), \\ f^{target\ SD} &= R_1(1 - R_4)R_2R_3, \\ f^{DD} &= R_1(1 - R_4)(1 - R_2), \\ f^{CD} &= R_1R_4. \end{aligned} \quad (4.1)$$

The predictions of these ratios are different among different models. For the R_1 case, the predictions are 0.074, 0.11, and 0.18 by SIBYLL 2.3c, QGSJET II-04, and EPOS-LHC, respectively, so the range of the predictions among models is 0.074-0.18. In this analysis, the range of the predictions among models is used as the realistic range of ratios. To estimate the effect of model discrepancies of these ratios, we changed the ratio within the range of predictions. Since one of the models does not have CD, we do not change R_4 .

$\langle X_{max} \rangle$ after modification of the ratio, $\langle X_{max}^{modified} \rangle$, is calculated by using the following equation:

$$\langle X_{max}^{modified} \rangle = \sum_i f^i \langle X_{max}^i \rangle, \quad (4.2)$$

where i is one of the categories of ND, projectile SD, target SD, DD, and CD. $\langle X_{max}^i \rangle$ is the $\langle X_{max} \rangle$ prediction of the category i , and f^i is the fraction of the category i after modification of one of the ratios. The results of $\langle X_{max}^{modified} \rangle$ are shown in Figure 3. When R_1 is shifted to the value of EPOS-LHC, $\langle X_{max}^{modified} \rangle$ increases by 3.2 g/cm² from the original $\langle X_{max} \rangle$ of QGSJET II-04. This is a 3.7 g/cm² increase in the case of SIBYLL 2.3c.

Finally, the maximum size of the effect for the ratio is estimated by using Equation 4.3:

$$E_{max}^{R_j} = \sum_i f_{R_j\ Max.}^i \langle X_{max}^i \rangle - \sum_i f_{R_j\ Min.}^i \langle X_{max}^i \rangle, \quad (4.3)$$

where $f_{R_j\ Max.}^i$ ($f_{R_j\ Min.}^i$) is the fraction when R_j is the maximum (minimum) within the range of predictions. The maximum effect $E_{max}^{R_1}$ is 5.05 g/cm², which is 18.4 % of the current size of the model discrepancy of $\langle X_{max} \rangle$ predictions and is non-negligible. $E_{max}^{R_2}$ and $E_{max}^{R_3}$ are 0.37 g/cm² and 0.19 g/cm², respectively, which is smaller than 1.5 % of the current model discrepancy and

is negligible. These analyses only consider the collision at the first interaction, so these results are underestimated. We extend the analysis to all hadronic collisions in the air shower in the next section.

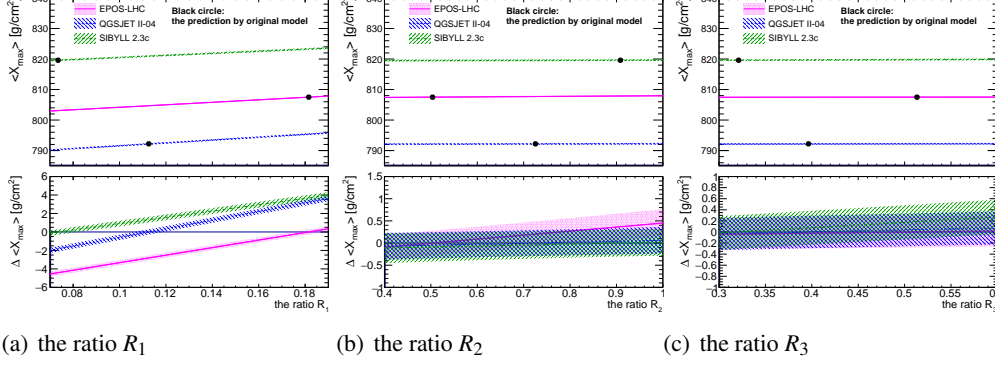


Figure 3: The ratio dependence of $\langle X_{max} \rangle$ for (a) the ratio R_1 , (b) R_2 , and (c) R_3 for EPOS-LHC (solid line), QGSJET II-04 (dashed line), and SIBYLL 2.3c (dash-dotted line). Hatched regions show statistical errors. The upper panel of each graph shows the $\langle X_{max} \rangle$ as a function of the ratio, and black circles show the predictions of the original model. The bottom panel shows $\Delta \langle X_{max} \rangle$, which is $\langle X_{max}^{original} \rangle - \langle X_{max}^{modified} \rangle$, where $\langle X_{max}^{original} \rangle$ is the prediction of the original model and $\langle X_{max}^{modified} \rangle$ is the modified prediction. The energy of a primary proton is 10^{19} eV.

4.2 The effect of the fraction of diffractive collisions in the air shower

To consider the effect of the ratio R_1 for all hadronic interactions in the air shower, we artificially changed the ratio of collision types by resampling the collision in the simulation. The procedure of resampling is as follows:

1. The ratio after resampling (the target ratio) is defined using the ratio simulated by CRMC.
2. When a hadronic collision with the concerning collision type is generated in the air shower, the output collision type is chosen randomly by following the target ratio. A collision is regenerated until a collision with the chosen collision type is generated.
3. Resampling is performed for all interactions above 10^{15} eV.

Figure 4 shows the ratio R_1 in the proton-Nitrogen and π^+ -Nitrogen collisions simulated by CRMC. Energy and the incidence particle dependence of the ratio R_1 are shown. The target of the ratio is defined by fitting predictions of EPOS-LHC to the equation $a \log_{10}(E) + b$ above 10^{15} eV. The target of the baryon incident collisions is a function fitted to proton-Nitrogen collisions, and that of the meson incident collisions is a function fitted to π^+ -Nitrogen collisions.

The air shower events with this resampling are simulated using CONEX 5.64. The number of events is 40,000. Table 1 shows the results of resampling of R_1 . The targets of the ratio are taken from EPOS-LHC, so the systematic uncertainty is estimated by comparing $\langle X_{max} \rangle$ predictions of the original simulation using EPOS-LHC and that after resampling using EPOS-LHC. The size of the effect of the resampling is 8.9 g/cm^2 for SIBYLL 2.3c and 4.4 g/cm^2 for QGSJET II-04, which

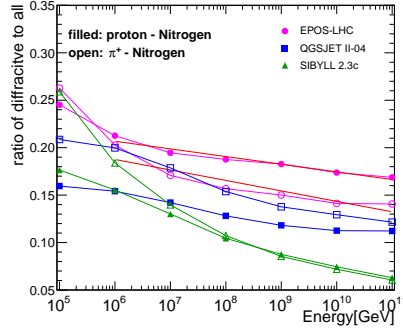


Figure 4: The ratio of diffractive collisions to all collisions (R_1) simulated by using CRMC v1.7 [10]. The ratio R_1 of EPOS-LHC is fitted by the equation $a \log_{10}(E) + b$ above 10^{15} eV (straight solid line).

Table 1: The effect of the ratio of diffractive collisions to all collisions in the air shower. The target of resampling is set by fitting the ratio of predictions by EPOS-LHC with energy above 10^{15} eV. The unit is g/cm^2 .

model	X_{max} [g/cm^2]		
	model original	with resampling	difference
EPOS-LHC	807.5 ± 0.3	809.5 ± 0.3	2.0 ± 0.4
QGSJET II-04	792.2 ± 0.3	796.6 ± 0.3	4.4 ± 0.4
SIBYLL 2.3c	819.6 ± 0.3	828.5 ± 0.3	8.9 ± 0.4
model discrepancy	27.4	31.9	

is 32.5 % and 16.1 % of the current size of the model discrepancy of $\langle X_{max} \rangle$ predictions. The systematic uncertainty is $2.0 \text{ g}/\text{cm}^2$, and the statistical uncertainty is $0.4 \text{ g}/\text{cm}^2$. These results mean that the effect of the ratio of R_1 is non-negligible. As discussed in the previous section, $\langle X_{max} \rangle$ becomes larger by 3.2 to 3.7 g/cm^2 when R_1 at the first interaction is shifted to the value of EPOS-LHC; therefore, the effect of changing fractions in the whole air shower is 1 to 2 times as large as that at the first interaction in the air shower. This feature indicates that the fraction of the first interaction is very important, and the fractions of the secondary interactions have non-negligible effects.

Table 1 denotes important information. The model discrepancy of the $\langle X_{max} \rangle$ prediction between EPOS-LHC and QGSJET II-04 decreases by $2.4 \text{ g}/\text{cm}^2$ after resampling, but that between EPOS-LHC and SIBYLL 2.3c increases by $6.9 \text{ g}/\text{cm}^2$. Therefore, the model discrepancies of $\langle X_{max} \rangle$ predictions among the three models increase by $4.5 \text{ g}/\text{cm}^2$ after resampling. These results mean that the ratio R_1 has a non-negligible effect on the $\langle X_{max} \rangle$ prediction; however, if the ratio R_1 of the three models is set to the same value after improvements, model discrepancies become larger.

5. Discussion and conclusion

In this study, we estimated the effect of diffractive collisions by focusing on the fraction of the collision types. The effect of the ratio of diffractive collisions to all inelastic collisions was 32.5 % of the current size of the model discrepancies of $\langle X_{max} \rangle$ predictions among models, which was

non-negligible. The effects of the ratios of the fraction among the diffractive collision types, for example, the ratio of SD to SD and DD, were smaller than 1.5 % of the current model discrepancy and were negligible. However, the $\langle X_{max} \rangle$ after resampling showed larger model discrepancies than the current one. These results mean that the effect of the fraction of diffractive collisions is one of the sources of model discrepancies, but not the main source of the current model discrepancy. Therefore, we need to consider other sources of the model discrepancy.

The model discrepancies of the fraction of projectile SD and DD were large, and these were the main sources of discrepancies of the ratio R_1 among models. These model discrepancies in the fraction of projectile SD and DD were also large at 10^{17} eV, which corresponds to the energy of nucleon-nucleon collisions in the Large Hadron Collider at CERN. It is important to measure these fractions by collider experiments for reducing the uncertainty of $\langle X_{max} \rangle$ predictions caused by the fraction of collision type.

Acknowledgements

We thank N. Sakurai for providing the programs for resampling in CONEX. We are grateful to F. Riehn for useful discussions and comments.

References

- [1] J. Bellido et al., *Depth of maximum of air-shower profiles at the Pierre Auger Observatory: Measurements above $10^{17.2}$ eV and Composition Implications*, PoS(ICRC2017) 506.
- [2] S.Ostapchenko, *LHC data on inelastic diffraction and uncertainties in the predictions for longitudinal extensive air shower development*, *Physical Review D* **89** (2014) 074009.
- [3] L. B. Arbeletche, V. P. Goncalves, and M. A.Muller, *Investigating the influence of diffractive interactions on ultra - high energy extensive air showers*, *International Journal of Modern Physics A* **33** (26) 01.
- [4] T. Bergmann et al., *One-dimensional hybrid approach to extensive air shower simulation*, *Astropart. Phys.***26**(2007) 420-432.
- [5] T. Pierog, I. Karpenko, J. M. Katzy, E. Yatsenko, and K. Werner, *EPOS LHC: Test of collective hadronization with data measured at the CERN Large Hadron Collider*, *Physical Review C* **92** (2015) 034906.
- [6] S. Ostapchenko, *Monte Carlo treatment of hadronic interactions in enhanced Pomeron scheme: I. QGSJET-II model*, *Physical Review D* **83** (2011) 014018.
- [7] E.-J. Ahn, R. Engel, T. K. Gaisser, P. Lipari, and T. Stanev, *Cosmic ray interaction event generator SIBYLL 2.1*, *Physical Review D* **80** (2009) 094003.
- [8] F. Riehn et al., *The hadronic interaction model Sibyll 2.3c and Feynman scaling*, PoS **ICRC2017** (2017) 301.
- [9] S.A. Bass et al., *Prog.Part.Nucl.Phys.* 41 (1998) 225; M. Bleicher et al., *J. Phys. G25* (1999) 1859.
- [10] T. Pierog, C. Baus, R. Ulrich, <https://web.ikp.kit.edu/rulrich/crmc.html>